European Review for Medical and Pharmacological Sciences 2019; 23: 7611-7618

MicroRNA-150 alleviates acute myocardial infarction through regulating cardiac fibroblasts in ventricular remodeling

H.-B. TIAN[1,2], S.-H. LI[2], K.-Q. HU[1], Y.-S. ZAN[2], X.-L. ZHANG[3], G.-H. SU[1]

[1]Department of Cardiology, Jinan Central Hospital Affiliated to Shandong University, Jinan, China
[2]Department of Cardiology, Shandong Provincial Hospital Affiliated to Shandong University, Jinan, China
[3]Department of Cardiology, Qingzhou People's Hospital, Qingzhou, China

Abstract. – OBJECTIVE: The aim of this study was to investigate the effect of microRNA-150 on the regulation of myocardial fibrosis and ventricular remodeling in rats with acute myocardial infarction (AMI).

MATERIALS AND METHODS: The AMI rats model was established by the ligation of the left anterior descending coronary artery (LAD) *in vivo.* After AMI procedures, the rats were injected with microRNA-150 lentivirus overexpression or negative control, respectively. Cardiac function of rats was evaluated by echocardiography. Hematoxylin and eosin (HE) staining and Masson trichrome were performed to evaluate myocardial fibrosis in each rat. Meanwhile, cardiomyocyte apoptosis was detected by terminal deoxynucleotidyl transferase (TdT)-mediated dUTP nick end labeling (TUNEL) method. The expression levels of microRNA-150, col1α1, col1α2, col3 and α smooth muscle actin (α-SMA) in the border zone of rat infarct myocardium were detected by quantitative Real Time-Polymerase Chain Reaction (qRT-PCR) and Western blot, respectively.

RESULTS: MicroRNA-150 expression in the border zone of infarct myocardium decreased significantly at day 28 after AMI ($p<0.05$). Overexpressing microRNA-150 significantly improved cardiac function, decreased collagen volume fraction (CVF) and attenuated cardiomyocyte apoptosis in rats. Furthermore, the expression levels of col1α1, col1α2, col3 and α-SMA in the border zone of infarct myocardium were remarkably down-regulated in rats overexpressing microRNA-150 compared with those of controls ($p<0.001$).

CONCLUSIONS: MicroRNA-150 expression in the border zone of rat infarct myocardium decreased at day 28 after AMI. In addition, the up-regulation of microRNA-150 in myocardial tissue could inhibit myocardial fibrosis and improve ventricular remodeling at post-AMI.

Key Words:
Acute myocardial infarction (AMI), MicroRNA-150, Myocardial fibrosis, Ventricular remodeling.

Introduction

Acute myocardial infarction (AMI) is a condition of acute ischemic necrosis of myocardial tissues. It is also a common critical emergency in internal medicine. AMI is the result of secondary thrombus due to rupture, erosion and endothelial damage of unstable coronary artery. Acute, persistent and complete occlusion of coronary arteries reduces or even interrupts blood flow, eventually leading to myocardial ischemia, injury, and necrosis[1,2].

Reperfusion therapies, such as thrombolysis, percutaneous transluminal coronary intervention (PCI), and coronary artery bypass graft surgery (CABG) have greatly improved the prognosis of AMI. However, many patients are still aggravated by heart failure due to ventricular remodeling at post-AMI[3]. Ventricular remodeling (VR) is an important pathological phenomenon in the progression of diseases from AMI to heart failure. It is manifested as hypertrophy and apoptosis of cardiomyocytes, excessive deposition of extracellular matrix (ECM), angiogenesis and inflammatory response[4,5]. Post-AMI myocardial fibrosis is a necessary part of VR. The main pathological changes of VR are ischemia-induced activation of cardiac fibroblasts (CFs) and the proliferation of a large number of ECM. This may result in an excessive deposition of ECM and changes in collagen composition[6]. At the initial stage of AMI, abundant ECM gradually deposits, thereby leading to increased cardiac contractility. However, it also forms scars to prevent heart rupture and improve heart function to some extent. With the deterioration of AMI, myocardial fibrosis induced by excessive deposition of ECM damages ventricular diastolic function. Ultimately, this

Corresponding Author: Guohai Su, MD; e-mail: gttstg@163.com

can induce malignant arrhythmia and even heart failure. Therefore, the prevention of excessive myocardial fibrosis, especially in the late stage of AMI, is necessary for AMI intervention[7].

MicroRNAs are a class of endogenous, short and non-coding RNAs with18-22 nucleotides in length. They are widely present in various organisms[8]. Due to the lack of an open reading frame, microRNAs do not have the ability to encode proteins. However, they can degrade or inhibit the translation of target mRNAs by binding to their 3'UTRs. Previously Gambari et al[9] have found that microRNAs are able to regulate important biological processes, such as cell proliferation, differentiation, apoptosis, and development. In recent years, the key roles of microRNAs in cardiovascular development and cardiac pathophysiology have been widely elucidated. Differentially expressed microRNAs have been identified in congenital heart disease, physiological or pathological cardiac hypertrophy and heart failure, showing their potential functions in VR[10-12]. For example, microRNA-208a inhibits myocardial fibrosis and improves cardiac function through regulating its target gene endoglin[13]. MicroRNA-208b regulates myocardial fibrosis at post-AMI through transcription factor GATA4[14]. MicroRNA-34a alleviates myocardial fibrosis in mice with myocardial infarction by acting on Smad4[15]. MicroRNA-150 has been found to be closely related to the occurrence and development of diabetic cardiomyopathy. Meanwhile, it regulates myocardial fibrosis in a diabetic cardiomyopathy model by affecting the secretion of collagen type 1 (col1)[16]. Deng et al[17] have found that microRNA-150 is downregulated in fibrotic myocardium induced by aortic arch constriction (TAC). However, upregulation of microRNA-150 expression in the myocardium markedly improves myocardial fibrosis by preventing the activation, proliferation, and transformation of cardiac fibroblasts into myofibroblasts *via* targeting c-Myb.

In this study, an AMI model was successfully established in rats. The aim of this work was to explore the effect of microRNA-150 on regulating cardiac fibroblasts and VR after AMI. Our findings might provide a novel direction for the prevention and treatment of VR at post-AMI.

Materials and Methods

Experimental Animals

Sixty healthy male Sprague-Dawley rats weighing 200-250 g were housed in a standard environment, with temperature of 20±2°C, relative humidity of 60-70%, and light/dark cycle for 12 h. All rats were randomly divided into three groups, sham group, negative control group (NC group, transfected with NC lentivirus), and microRNA-150 group (transfected with lentivirus overexpressing microRNA-150). Each group had 20 rats. This investigation was approved by the Animal Ethics Committee of Jinan Central Hospital Affiliated to Shandong University Animal Center.

Establishment of AMI Model in Rats

Rats were first anesthetized by intraperitoneal injection of 10% chloral hydrate (3 mL/kg). After fixation on the operating platform at a supine position, a longitudinal incision was made to expose the heart. Left anterior descending coronary artery (LAD) ligation was performed between the left atrial appendage and the pulmonary artery. Pale left ventricular wall, decreased ventricular wall motion and elevated ST-segment indicated the successful establishment of AMI model in rats. Rats in sham group were sutured in the same part, without LAD ligation. Subsequently, the rats were observed for about 20 min, and 1×10^7 TU lentivirus was injected 2 mm around the infarct myocardium per rat. The thoracic cavity was sutured layer by layer. Finally, the chest skin wound was applied with sodium penicillin powder after procedures.

After the procedures, rats were intraperitoneally injected with penicillin 100,000 units/day for three consecutive days to prevent infection.

Echocardiography in Rats

On the 28th day after LAD ligation, the rats were intraperitoneally injected with 4% of chloral hydrate (0.65 mL/kg). After the righting response disappeared, rat incisors and limbs were fixed in a supine position. M-mode echocardiograph was performed using a small-animal ultrasound probe (model Vevo 2100) on the long axis of the left ventricle. Left ventricular end-systolic dimension (LVESD), left ventricular end-diastolic dimension (LVEDD), left ventricular ejection fraction (LVEF) and left ventricular fractional shortening (LVFS) were recorded.

Sample Collection

After echocardiography was performed, the rats were sacrificed. The border zone of myocardial infarction was harvested. After washing with pre-cooled saline solution, part of the myocardial tissues was preserved at −80°C for use. Meanwhile, the rest of tissues was fixed in 4% of paraformaldehyde for pathological examination.

Terminal Deoxynucleotidyl Transferase (TdT)-Mediated dUTP Nick End Labeling (TUNEL)

Myocardial tissues were first dehydrated and embedded. Then, the sections were routinely dewaxed, washed, hydrated and fixed strictly in accordance with TUNEL apoptosis kit (Sigma-Aldrich, St. Louis, MO, USA). Five fields were randomly selected for each sample. The apoptosis of cells was observed, and at least 100 cells were counted in each field (magnification 400×). AI = number of apoptotic cells / total number of cells × 100%.

Myocardial Histopathological Staining

Myocardial tissue in the infarct border zone was first fixed in 4% of paraformaldehyde for 24 h, embedded in paraffin and sectioned. After dewaxing and hydration, the sections were stained with hematoxylin-eosin. For Masson trichrome, the sections were stained with Weigert's iron hematoxylin working solution, and color separated in 5% of hydrochloric acid solution. After that, the sections were further stained with 0.5% of Biebrich scarlet-acid fuchsin solution for 10-20 s. Subsequently, the sections were dehydrated, cleared in xylene and mounted. Cardiomyocytes were stained red, whereas collagen fibers were stained blue with a cord-like structure. Collagen fibers were distributed in the intercellular space. Finally, collagen volume fraction (CVF) was calculated using the Image-Pro Plus software.

Western Blot

Radioimmunoprecipitation assay (RIPA) protein lysate (Beyotime, Shanghai, China) was used to extract the total protein in tissues of each group of tissues. The concentration of extracted protein was determined by the bicinchoninic acid (BCA). Protein samples were electrophoresed on polyacrylamide gels and transferred onto polyvinylidene difluoride (PVDF) membranes (Merck Millipore, Billerica, MA, USA). After blocking with 5% of skimmed milk, the membranes were incubated with primary antibody (Cell Signaling Technology, Danvers, MA, USA) at 4°C overnight. On the next day, the membranes were incubated with corresponding secondary antibody after rinsing with Tris-Buffered Saline and Tween 20 solution (TBST). Enhanced chemiluminescence (ECL) was used to expose protein bands on the membrane. Integral optical density was analyzed by the gel imaging analysis system. Glyceraldehyde 3-phosphate dehydrogenase (GAPDH) was used as an internal reference.

Quantitative Real Time-Polymerase Chain Reaction (qRT-PCR)

Total RNA in myocardial tissues or cells were extracted using TRIzol (Invitrogen, Carlsbad, CA, USA). After reverse transcription into complementary deoxyribose nucleic acid (cDNA), qRT-PCR was performed to amplify target genes. The mRNA expression levels of microRNA-150, col1α1, col1α2, col3 and α smooth muscle actin (α-SMA) were calculated. QRT-PCR reaction conditions were as follows: 94°C for 30 s, 55°C for 30 s and 72°C for 90 s, for a total of 40 cycles. The relative expression level of target genes was expressed by the $2^{-\Delta\Delta Ct}$ method. Primer sequences used in this study were as follows: microRNA-150, F: 5'-GCCTAATTATCCGGACTG-3', R: 5'-GATTGTGTCGTGGCCCG-3'; col1α1, F: 5'-AGCACCGCATTTGAACAA-3', R: 5'-GCGTGCCAATAGCTTCAGTTCT-3'; col1α2, F: 5'-GTGAATGATAGTGAGGAC-3', R: 5'-TGAACGATTTGCCACACAA-3'; col3, F: 5'-CGCTGCAGCTGGAGAGTGC-3', R: 5'-TGTGCTCTGCTGAGAGGTGGA-3'; α-SMA, F: 5'-ACGGATGCACGCTGTACGAT-3', R: 5'-CGTCTTTCAACCGCAGGAGCA-3'; β-actin: F: 5'-CCTGGCACCCAGCACAAT-3', R: 5'-GCTGATCCACATCTGCTGGAA-3'.

Statistical Analysis

Statistical Product and Service Solutions (SPSS) 17.0 statistical software (SPSS Inc., Chicago, IL, USA) was used for all statistical analysis. Quantitative data were represented as mean ± standard deviation ($\bar{x}\pm s$). Categorical data and measurement data were analyzed by Chi-square test and *t*-test, respectively. $p<0.05$ was considered statistically significant.

Results

Heart Function of AMI Rats

M-mode ultrasound showed normal systolic myocardial contractility in rats of sham group (Figure 1A-a). Compared with sham group, the myocardial contractile function of the left ventricular anterior wall in rats of NC group and microRNA-150 group was significantly worse. However, anterior wall myocardial contractility was stronger in microRNA-150 group than NC group (Figure 1A-bc). LVEF and LVFS decreased remarkably in NC and microRNA-150 group relative to sham group. Moreover, LVEF and LVFS in microRNA-150 group were significantly higher than NC group ($p<0.05$, Figure 1A-de).

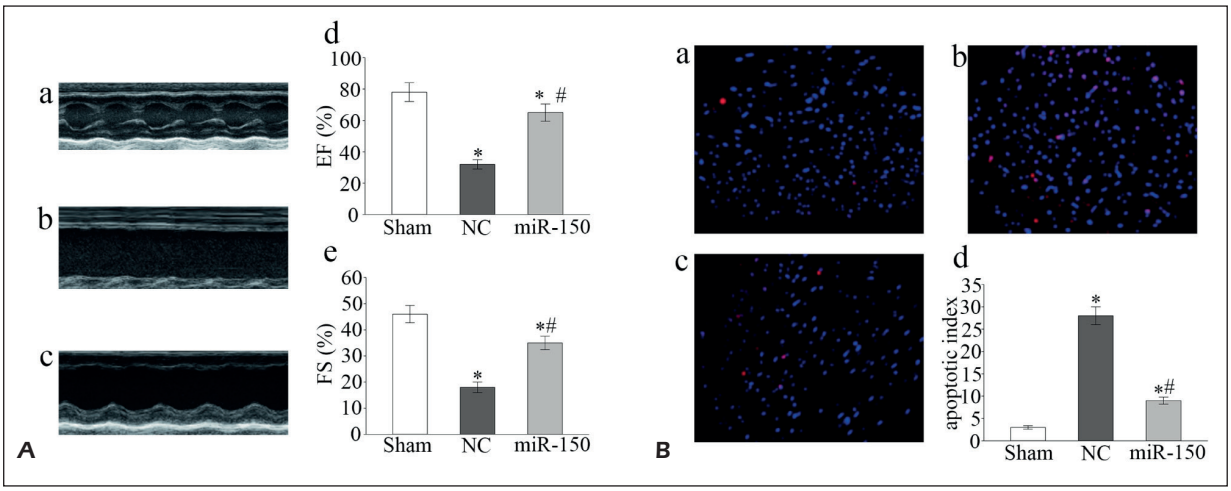

Figure 1. A, Heart function of AMI rats. a, M-mode ultrasound in rats of sham group. b, M-mode ultrasound in rats of NC group. c, M-mode ultrasound in rats of miR-150 group. d, LVEF in rats of sham group, NC group and miR-150 group. e, LVFS in rats of sham group, NC group and miR-150 group. **B**, Cardiomyocyte apoptosis in the border zone of infarct myocardium (Magnification: 400x). a, Apoptosis of rat cardiomyocytes in sham group. b, Apoptosis of rat cardiomyocytes in NC group. c, Apoptosis of rat cardiomyocytes in miR-150 group. d, Comparison of apoptotic index among sham group, NC group and miR-150 group. *$p<0.05$ *vs.* sham group, $^{\#}p<0.05$ *vs.* NC group.

Cardiomyocyte Apoptosis in the Border Zone of Infarct Myocardium

Only a few apoptotic cells were observed in myocardial tissues of rats in sham group. The number of apoptotic cardiomyocytes increased significantly in NC group. Meanwhile, less apoptotic cardiomyocytes were observed in microRNA-150 group when compared with NC group (Figure 1B-abc).

Myocardial Histopathological Staining of AMI Rats

HE staining images revealed an orderly arrangement of cardiomyocytes with similar nuclear size (Figure 2A-a). Disordered cardiomyocytes, abnormal nucleus aggregation and uneven size and shape of the nucleus were significantly pronounced in NC group (Figure 2A-b). However, microRNA-150 group showed a small number of

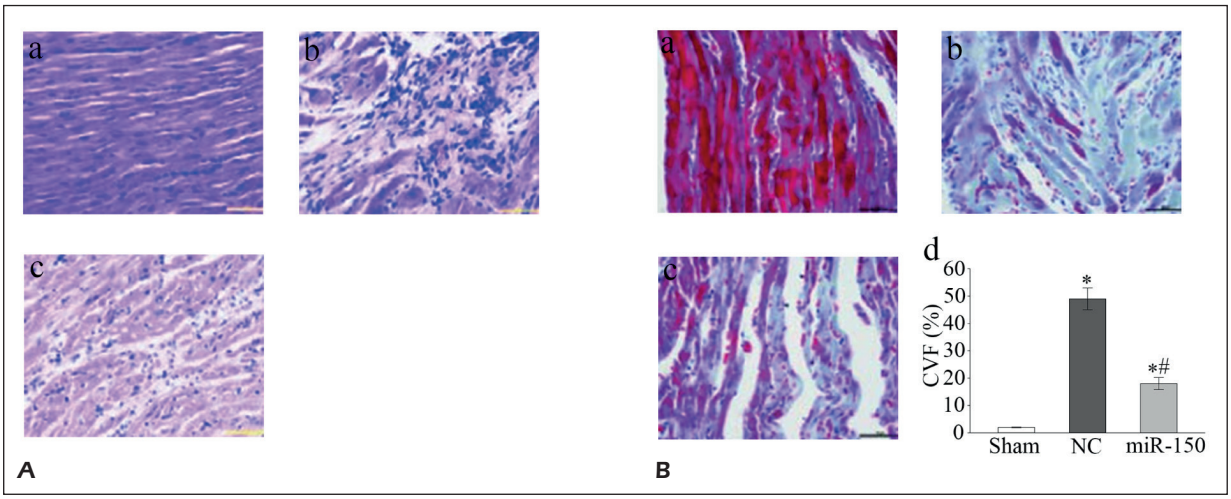

Figure 2. Myocardial histopathological staining of AMI rats (Magnification: 400x). **A**, a, Morphology of rat cardiomyocytes in sham group. b, Morphology of rat cardiomyocytes in NC group. c, Morphology of rat cardiomyocytes in miR-150 group. **B**, a, Cardiac fibrosis in rats of sham group. b, Cardiac fibrosis in rats of NC group. c, Cardiac fibrosis in rats of miR-150 group. d, CVF in rats of sham group, NC group and miR-150 group. *$p<0.05$ *vs.* sham group, $^{\#}p<0.05$ *vs.* NC group.

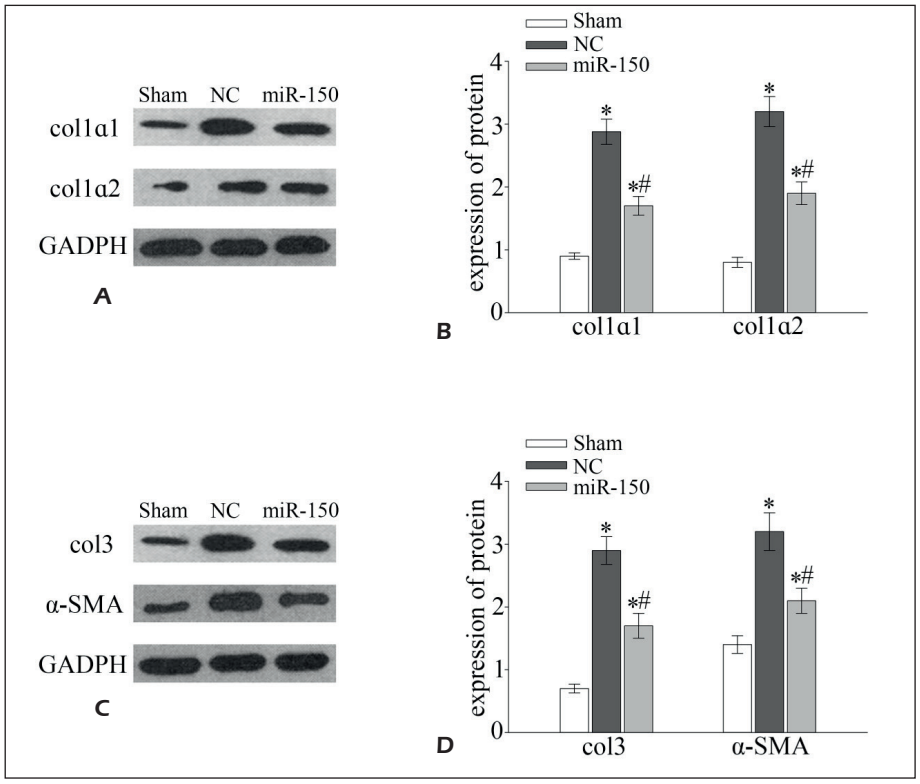

Figure 3. Protein levels of myocardial fibrosis-related genes in the border zone of infarct myocardium. **A**, Western blot analyses of col1α1 and col1α2 in sham group, NC group and miR-150 group. **B**, Protein levels of col1α1 and col1α2 in sham group, NC group and miR-150 group. C, Western blot analyses of col3 and α-SMA in sham group, NC group and miR-150 group. D, Protein levels of col3 and α-SMA in sham group, NC group and miR-150 group. *p<0.05 *vs.* sham group, #p<0.05 *vs.* NC group.

disordered cardiomyocytes with basically similar nucleus size and morphology (Figure 2A-c).

Masson trichrome images showed that sham group and NC group presented the least and most blue collagens, respectively (Figure 2B-abc). CVF was calculated by image analysis software after Masson trichrome. The results indicated that CVF was the highest in NC group and lowest in sham group (p<0.05, Figure 2B-d).

The Protein Levels of Myocardial Fibrosis Related Genes in the Border Zone of Infarct Myocardium

Compared with sham group, the protein levels of col1α1, col1α2, col3, and α-SMA in the border zone of rat infarct myocardium increased significantly in microRNA-150 group and NC group (p<0.05). However, the protein expressions of these indicators were significantly down-regulated in microRNA-150 group relative to NC group (p<0.05, Figure 3A-3D).

The mRNA Levels of Myocardial Fibrosis-Related Genes in the Border Zone of Infarct Myocardium

The mRNA expression level of microRNA-150 was markedly up-regulated in microRNA-150 group, confirming successful administration of lentivirus overexpressing microRNA-150 (Figure 4A). The mRNA levels of col1α1, col3, and α-SMA in the border zone of rat infarct myocardium were remarkably higher in microRNA-150 group and NC group than sham group (p<0.05). In particular, the mRNA levels of these indicators were remarkably lower in microRNA-150 group compared with NC group (p<0.05, Figure 4B-4D).

Discussion

A series of compensatory mechanisms can be activated after AMI, involving cardiomyocytes, cardiac fibroblasts, ECM, etc. Lack of proper intervention and treatment for AMI lead to poor VR and even progress to heart failure[18]. The progression of heart failure is closely related to myocardial pathological processes, including poor VR, cardiomyocyte hypertrophy, apoptosis, and myocardial fibrosis[19,20]. In ischemic heart disease, fibrosis in non-infarcted myocardium is a major determinant of progressive VR[21].

The main feature of myocardial fibrosis is the excessive accumulation of ECM such as collagen fibers. It is also the advanced pathological manifestation of various cardiovascular diseases, including AMI, hypertension, diabetic cardiomyopathy

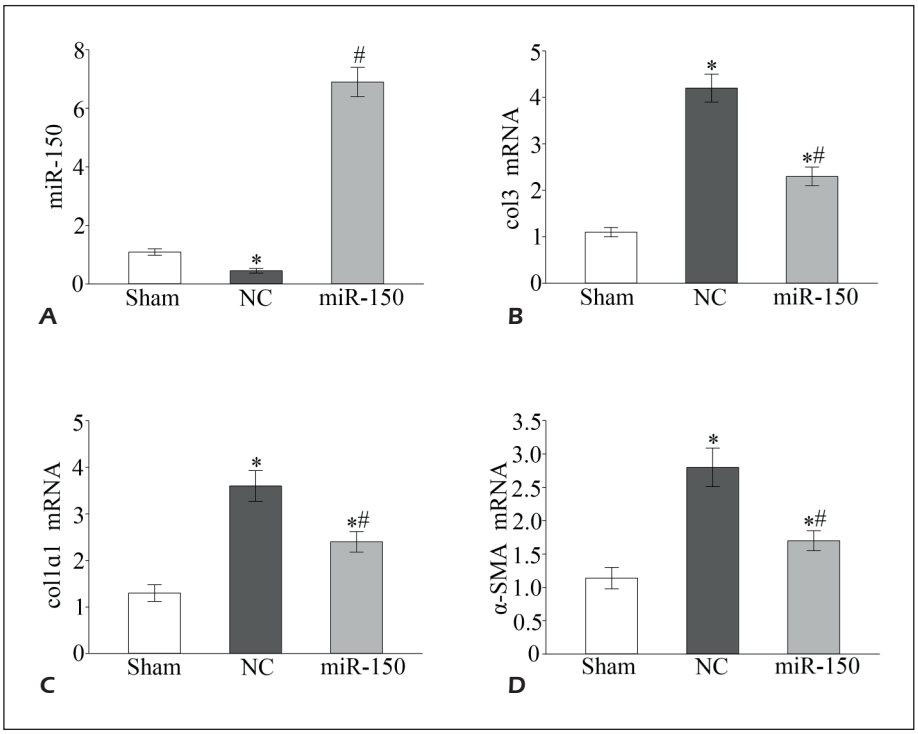

Figure 4. The mRNA levels of myocardial fibrosis-related genes in the border zone of infarct myocardium. **A**, The mRNA level of miR-150 in sham group, NC group and miR-150 group. **B**, The mRNA level of col1α1 in sham group, NC group and miR-150 group. **C**, The mRNA level of col3 in sham group, NC group and miR-150 group. **D**, The mRNA level of α-SMA in sham group, NC group and miR-150 group. *$p<0.05$ *vs.* sham group, #$p<0.05$ *vs.* NC group.

and pulmonary hypertension[22]. Typically, cardiac fibroblasts are activated, proliferated and transformed into myofibroblasts expressing α-SMA. This may further synthesize and secrete a large number of ECM[23,24]. The cardiac extracellular matrix is composed of a variety of structural, matricellular and adhesion proteins synthesized and secreted by cells. It not only provides a structural framework for cardiomyocytes, but also inhibits the transmission of electrocardiographic activity by regulating various bio-signal molecules[25]. Among them, collagen type 1 (colα1) and colα3 are two main structural proteins of ECM. α-SMA is a typical marker for the transformation of cardiac fibroblasts into myofibroblasts[26]. Therefore, col1α1, col1α2, col3, and α-SMA are commonly used as measurement indicators for evaluating the severity of myocardial fibrosis.

MicroRNAs are non-coding RNAs without protein-encoding functions. They can regulate gene expression through binding to target mRNAs, thereby participating in various biological progresses[27]. In recent years, some certain microRNAs have been confirmed to participate in the fibrosis process by inhibiting synthesis and deposition of ECM, as well as regulating fibrosis-related pathways. These microRNAs are widely involved in hypertension, myocardial ischemia, myocardial ischemia, and other cardiovascular diseases[28-30]. MicroRNA-150 contains approximately 22 nucleotides in length. Meanwhile, it is abundantly expressed in lymphocytes and monocytes. Previous studies[31-33] have reported that microRNA-150 is associated with tumors, systemic scleroderma, tissue and organ fibrosis, and pulmonary hypertension. Recently, the relation between microRNA-150 and AMI has attracted increasingly more attention. MicroRNA-150 is abnormally expressed in myocardial infarction models, which can be used as an early diagnostic biomarker and prognostic indicator for AMI[34,35].

In this study, we found that miRNA-150 was downregulated in the border zone of infarct myocardium at day 28 after AMI. This was consistent with the results of Zeller et al[36,37]. After the inflammatory phase of AMI, fibroblasts proliferate and activate into myofibroblasts, thereby synthesizing and secreting a large number of ECM. In this research, we examined myocardial tissues of rats at day 28 after AMI, when tissue hyperplasia and scar formation were pronounced. During this period, inflammatory cells such as monocytes were not markedly infiltrated. Meanwhile, the expression of microRNA-150 decreased significantly. Notably, echocardiography and histopathological staining indicated significantly improved heart function of AMI rats

overexpressing microRNA-150. Overexpression of microRNA-150 could prevent myocardial fibrosis after AMI, and downregulate the expressions of col1α1, col1α2, col3, α-SMA in the border zone of infarct myocardium. These findings suggested that microRNA-150 overexpression in the border zone of infarct myocardium protected the myocardial injury and improved VR. Our results provided new directions for gene therapy of AMI.

In summary, microRNA-150 can inhibit myocardial fibrosis and improve ventricular remodeling after AMI, which brings hope for improving the clinical outcomes of AMI.

Conclusions

MicroRNA-150 expression in the border zone of rat infarct myocardium decreased at 28 days after AMI. Furthermore, upregulation of microRNA-150 expression in myocardial tissue could inhibit myocardial fibrosis and improve ventricular remodeling at post-AMI.

Conflict of Interests

The authors declared that they have no conflict of interests.

References

1) Reed GW, Rossi JE, Cannon CP. Acute myocardial infarction. Lancet 2017; 389: 197-210.
2) Snorrason EL, Johannnesdottir BK, Aspelund T, Gudnason V, Andersen K. [Long-term survival of patients with acute myocardial infarction in Iceland]. Laeknabladid 2018; 104: 491-497.
3) Yang CJ, Chen PC, Lin CS, Tsai CL, Tsai SH. Thrombolytic therapy-associated acute myocardial infarction in patients with acute ischemic stroke: a treatment dilemma. Am J Emerg Med 2017; 35: 801-804.
4) Fujisue K, Sugamura K, Kurokawa H, Matsubara J, Ishii M, Izumiya Y, Kaikita K, Sugiyama S. Colchicine improves survival, left ventricular remodeling, and chronic cardiac function after acute myocardial infarction. Circ J 2017; 81: 1174-1182.
5) Ali M, Pulli B, Courties G, Tricot B, Sebas M, Iwamoto Y, Hilgendorf I, Schob S, Dong A, Zheng W, Skoura A, Kalgukar A, Cortes C, Ruggeri R, Swirski FK, Nahrendorf M, Buckbinder L, Chen JW. Myeloperoxidase inhibition improves ventricular function and remodeling after experimental myocardial infarction. JACC Basic Transl Sci 2016; 1: 633-643.
6) Xia J, Qu Y, Yin C, Xu D. Preliminary study of beta-blocker therapy on modulation of interleukin-33/ST2 signaling during ventricular remodeling after acute myocardial infarction. Cardiol J 2017; 24: 188-194.
7) Hendriks T, Hartman MHT, Vlaar PJJ, Prakken NHJ, van der Ende YMY, Lexis CPH, van Veldhuisen DJ, van der Horst ICC, Lipsic E, Nijveldt R, van der Harst P. Predictors of left ventricular remodeling after ST-elevation myocardial infarction. Int J Cardiovasc Imaging 2017; 33: 1415-1423.
8) Lekchnov EA, Zaporozhchenko IA, Morozkin ES, Bryzgunova OE, Vlassov VV, Laktionov PP. Protocol for miRNA isolation from biofluids. Anal Biochem 2016; 499: 78-84.
9) Gambari R, Brognara E, Spandidos DA, Fabbri E. Targeting oncomiRNAs and mimicking tumor suppressor miRNAs: new trends in the development of miRNA therapeutic strategies in oncology (Review). Int J Oncol 2016; 49: 5-32.
10) Grabmaier U, Clauss S, Gross L, Klier I, Franz WM, Steinbeck G, Wakili R, Theiss HD, Brenner C. Diagnostic and prognostic value of miR-1 and miR-29b on adverse ventricular remodeling after acute myocardial infarction - the SITAGRAMI-miR analysis. Int J Cardiol 2017; 244: 30-36.
11) Li AL, Lv JB, Gao L. MiR-181a mediates Ang II-induced myocardial hypertrophy by mediating autophagy. Eur Rev Med Pharmacol Sci 2017; 21: 5462-5470.
12) Yang X, Qin Y, Shao S, Yu Y, Zhang C, Dong H, Lv G, Dong S. MicroRNA-214 inhibits left ventricular remodeling in an acute myocardial infarction rat model by suppressing cellular apoptosis via the phosphatase and tensin homolog (PTEN). Int Heart J 2016; 57: 247-250.
13) Shyu KG, Wang BW, Cheng WP, Lo HM. MicroRNA-208a increases myocardial endoglin expression and myocardial fibrosis in acute myocardial infarction. Can J Cardiol 2015; 31: 679-690.
14) Zhou C, Cui Q, Su G, Guo X, Liu X, Zhang J. MicroRNA-208b alleviates post-infarction myocardial fibrosis in a rat model by inhibiting GATA4. Med Sci Monit 2016; 22: 1808-1816.
15) Huang Y, Qi Y, Du JQ, Zhang DF. MicroRNA-34a regulates cardiac fibrosis after myocardial infarction by targeting Smad4. Expert Opin Ther Targets 2014; 18: 1355-1365.
16) Costantino S, Paneni F, Lüscher TF, Cosentino F. MicroRNA profiling unveils hyperglycaemic memory in the diabetic heart. Eur Heart J 2016; 37: 572-576.
17) Deng P, Chen L, Liu Z, Ye P, Wang S, Wu J, Yao Y, Sun Y, Huang X, Ren L, Zhang A, Wang K, Wu C, Yue Z, Xu X, Chen M. MicroRNA-150 inhibits the activation of cardiac fibroblasts by regulating c-Myb. Cell Physiol Biochem 2016; 38: 2103-2122.
18) Bhatt AS, Ambrosy AP, Velazquez EJ. Adverse remodeling and reverse remodeling after myocardial infarction. Curr Cardiol Rep 2017; 19: 71.
19) Seropian IM, Toldo S, Van Tassell BW, Abbate A. Anti-inflammatory strategies for ventricular remodeling following ST-segment elevation acute myocardial infarction. J Am Coll Cardiol 2014; 63: 1593-1603.
20) Francis Stuart SD, De Jesus NM, Lindsey ML, Ripplinger CM. The crossroads of inflammation, fibrosis, and arrhythmia following myocardial infarction. J Mol Cell Cardiol 2016; 91: 114-122.

21) Reichert K, Pereira Do Carmo HR, Galluce Torina A, Diógenes de Carvalho D, Carvalho Sposito A, de Souza Vilarinho KA, da Mota Silveira-Filho L, Martins de Oliveira PP, Petrucci O. Atorvastatin improves ventricular remodeling after myocardial infarction by interfering with collagen metabolism. PLoS One 2016; 11: e0166845.
22) Talman V, Ruskoaho H. Cardiac fibrosis in myocardial infarction-from repair and remodeling to regeneration. Cell Tissue Res 2016; 365: 563-581.
23) Prabhu SD, Frangogiannis NG. The biological basis for cardiac repair after myocardial infarction: from inflammation to fibrosis. Circ Res 2016; 119: 91-112.
24) Shinde AV, Frangogiannis NG. Fibroblasts in myocardial infarction: a role in inflammation and repair. J Mol Cell Cardiol 2014; 70: 74-82.
25) Frangogiannis NG. Fibroblasts and the extracellular matrix in right ventricular disease. Cardiovasc Res 2017; 113: 1453-1464.
26) Tang CM, Zhang M, Huang L, Hu ZQ, Zhu JN, Xiao Z, Zhang Z, Lin QX, Zheng XL, Yang M, Wu SL, Cheng JD, Shan ZX. CircRNA_000203 enhances the expression of fibrosis-associated genes by derepressing targets of miR-26b-5p, Col1a2 and CTGF, in cardiac fibroblasts. Sci Rep 2017; 7: 40342.
27) Rupaimoole R, Slack FJ. MicroRNA therapeutics: towards a new era for the management of cancer and other diseases. Nat Rev Drug Discov 2017; 16: 203-222.
28) Liu X, Xu Y, Deng Y, Li H. MicroRNA-223 regulates cardiac fibrosis after myocardial infarction by targeting RASA1. Cell Physiol Biochem 2018; 46: 1439-1454.
29) Yuan J, Chen H, Ge D, Xu Y, Xu H, Yang Y, Gu M, Zhou Y, Zhu J, Ge T, Chen Q, Gao Y, Wang Y, Li X, Zhao Y. Mir-21 promotes cardiac fibrosis after myocardial infarction via targeting Smad7. Cell Physiol Biochem 2017; 42: 2207-2219.
30) Piccoli MT, Bär C, Thum T. Non-coding RNAs as modulators of the cardiac fibroblast phenotype. J Mol Cell Cardiol 2016; 92: 75-81.
31) Yuan G, Zhao Y, Wu D, Gao Ch. Mir-150 Up-regulates Glut1 and increases glycolysis in osteosarcoma cells. Asian Pac J Cancer Prev 2017; 18: 1127-1131.
32) Wang L, Xi Y, Sun C, Zhang F, Jiang H, He Q, Li D. CDK3 is a major target of miR-150 in cell proliferation and anti-cancer effect. Exp Mol Pathol 2017; 102: 181-190.
33) Wang W, Wang X, Zhang Y, Wang D, Gao H, Wang L, Gao S. Prognostic role of microRNA-150 in various carcinomas: a meta-analysis. Onco Targets Ther 2016; 9: 1371-1379.
34) Wu T, Wu D, Wu Q, Zou B, Huang X, Cheng X, Wu Y, Hong K, Li P, Yang R, Li Y, Cheng Y. Knockdown of long non-coding RNA-ZFAS1 protects cardiomyocytes against acute myocardial infarction via anti-apoptosis by regulating miR-150/CRP. J Cell Biochem 2017; 118: 3281-3289.
35) Ranganathan P, Jayakumar C, Tang Y, Park KM, Teoh JP, Su H, Li J, Kim IM, Ramesh G. MicroRNA-150 deletion in mice protects kidney from myocardial infarction-induced acute kidney injury. Am J Physiol Renal Physiol 2015; 309: F551-F558.
36) Zeller T, Keller T, Ojeda F, Reichlin T, Twerenbold R, Tzikas S, Wild PS, Reiter M, Czyz E, Lackner KJ, Munzel T, Mueller C, Blankenberg S. Assessment of microRNAs in patients with unstable angina pectoris. Eur Heart J 2014; 35: 2106-2114.
37) Goren Y, Meiri E, Hogan C, Mitchell H, Lebanony D, Salman N, Schliamser JE, Amir O. Relation of reduced expression of MiR-150 in platelets to atrial fibrillation in patients with chronic systolic heart failure. Am J Cardiol 2014; 113: 976-981.